

# Deactivation of the signal amplification by reversible exchange catalysis, progress towards *in vivo* application

Ryan E. Mewis, Marianna Fekete, Gary G. R. Green, Adrian C. Whitwood and Simon B. Duckett\*

*Centre for Hyperpolarisation in Magnetic Resonance, University of York, Heslington, York, YO10 5NY, UK. Tel +44 1904 432564; Email: simon.duckett@york.ac.uk*

## Contents

1. General .....	2
2. Characterisation data for 3 .....	3
3. UV-vis data of 2 and 3 .....	5
4. Selective NOESY data for $[\text{Ir}(\text{IMes})(\text{H})_2(\text{bpy})\text{L}^2]^+$ .....	6
5. UV-vis data for the addition of bpy to solution containing $\text{L}^2$ and 1 .....	6
6. Addition of 1,10-phenanthroline to a sample consisting of 1 and pyridine .....	7
7. References .....	9

## 1. General

$\text{Ir}(\text{IMes})(\text{COD})\text{Cl}$ , **1**, was synthesised as previously described.[1] Nicotinamide ( $\text{L}^1$ ), pyridine ( $\text{L}^2$ ), 1,10-phenanthroline and deuterated methanol were purchased from Sigma-Aldrich and used as received.

NMR samples consisted of **1** and  $\text{L}^1$  or  $\text{L}^2$  in a ratio of 1 : 8, and we made up in 0.6 ml of deuterated methanol (Young's capped NMR tube experiments) or 3 ml when an NMR flow system experiment was undertaken. Young's capped NMR tubes were degassed three times on a Schlenk line whilst immersing the solution in a dry  $\text{CO}_2$ / acetone slush bath. *Parahydrogen* was introduced into the NMR tube using a home-built generator; the *parahydrogen* had been formed by cooling the dihydrogen gas to 36 K over a bed of  $\text{Fe}_2\text{O}_3$ . For the flow measurements, the *parahydrogen* was supplied by a Bruker *parahydrogen* generator.

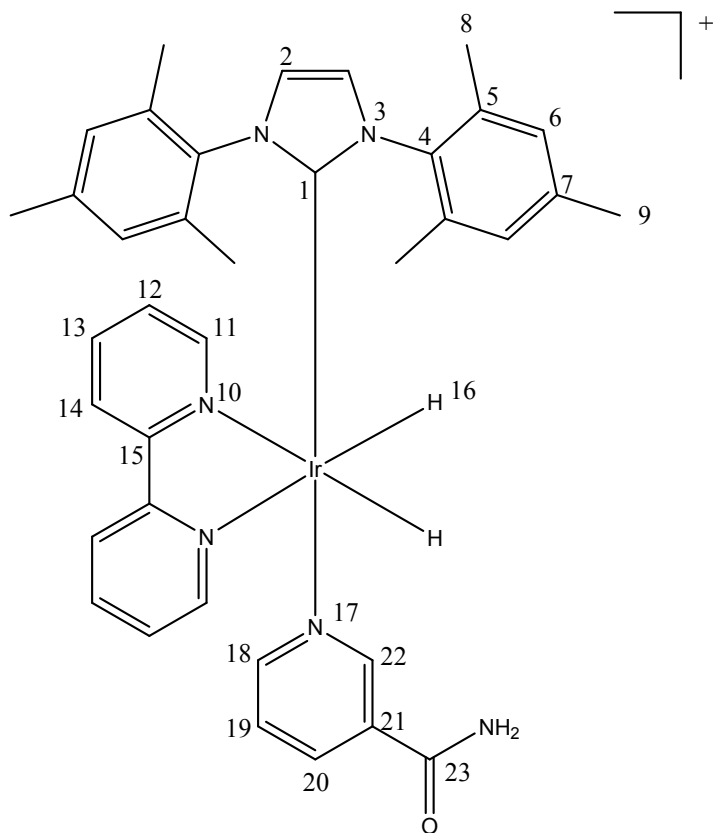
For hyperpolarisation experiments, *parahydrogen* was either bubbled through the solution for 10-20 s (flow measurements) or shaken in the fringe field of the spectrometer magnet for 10 s. The magnetic field experienced by the sample during the *parahydrogen* transfer process was either measured using a Hall probe, or precisely controlled in the vertical direction by a copper coil as described previously.[2]

NMR data was collected on a Bruker Advance III NMR spectrometer (9.4 T) that was fitted with a broad band inverse probe (BBI) or a flow probe at 298 K unless specified otherwise.

The NMR signal enhancement values were calculated by comparing the integrals of the thermal peaks for the specified protons of  $\text{L}^1$  (or  $\text{L}^2$ ) to those observed after hyperpolarisation transfer at the indicated magnetic field. The results are not corrected for relaxation losses during the transfer time (2.9 s for flow measurements and  $\approx$  4 s for Young's capped NMR tube experiments) into the magnet and hence reflect experimentally observed values.

Single crystals of **3** ( $\text{C}_{48}\text{H}_{51}\text{BF}_4\text{IrN}_5$ ) were grown from  $d_6$ -benzene solution. A suitable crystal was selected and placed in oil on micromount, on a SuperNova, Dual, Cu at zero, Eos diffractometer. The crystal was kept at 110.05(10) K during data collection. Using Olex2 [3], the structure was solved with the Superflip [4] structure solution program using Charge Flipping and refined with the ShelXL [5] refinement package using Least Squares minimisation.

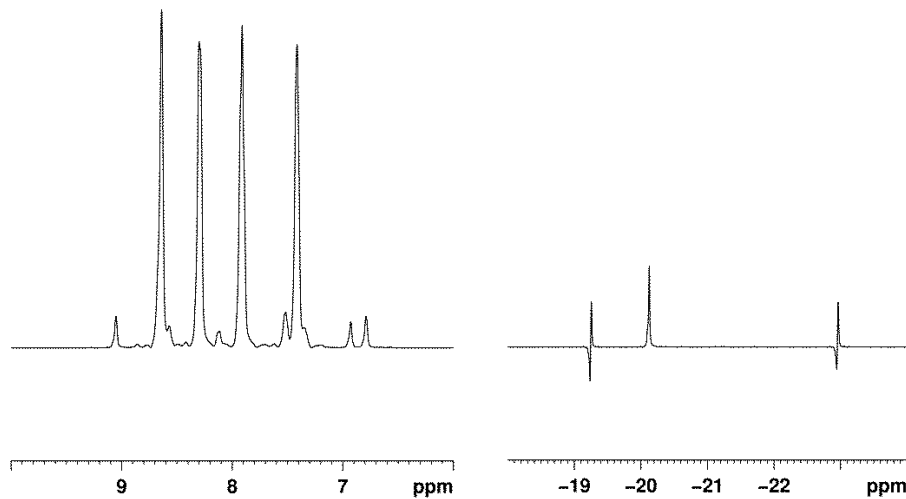
## 2. Characterisation data for cation 3



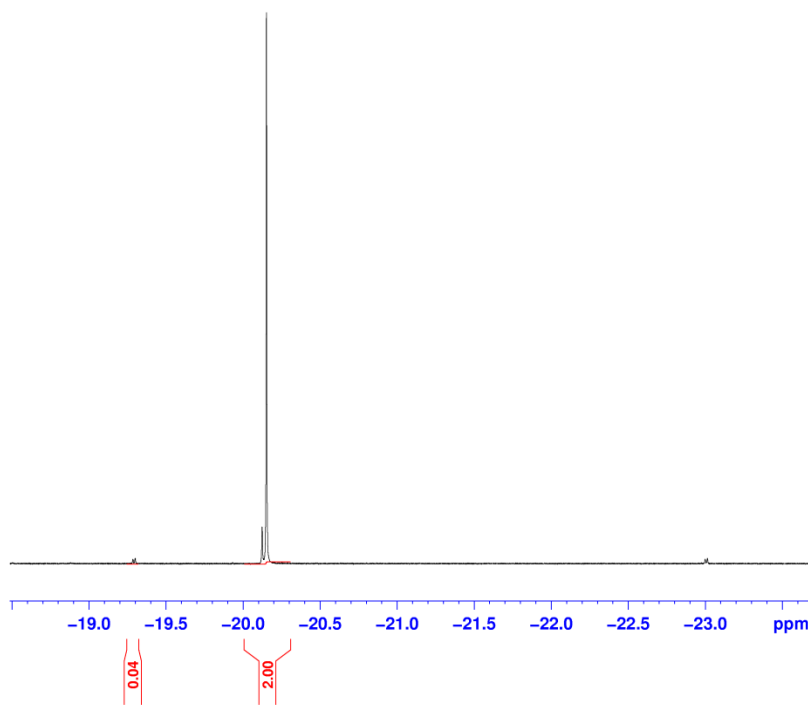
sTable 1: NMR chemical shift and specific spin-spin coupling data for **3**, collected in MeOH-*d*<sub>4</sub> solution at 253 K.

Atom number	<sup>1</sup> H δ /ppm	<i>J</i> <sub>HH</sub> / Hz	<sup>13</sup> C δ /ppm	<sup>15</sup> N δ /ppm
1			186.4	
2	6.97 (s)		122.5	
3				209
4			137.3	
5			135.9	
6	6.87 (s)		128.8	
7			138.7	
8	1.88 (s)		17.0	
9	2.36 (s)		19.7	
10				268
11	8.58 (d)	5.4	155.6	
12	7.39 (dd)	8.0, 5.4	127.3	
13	8.00 (dd)	8.3, 8.0	136.8	
14	8.20 (d)	8.3	123.1	
15			156.8	
16	-20.15 (s)			
17				241
18	8.36 (dt)	6.0, 1.2	155.8	
19	7.00 (dd)	8.0, 6.0	124.5	
20	7.96 (d)	8.0	134.8	
21			130.7	
22	8.63 (d)	1.2	153.1	
23			166.4	

(b)



(a)



sFigure 1. (a) NMR spectrum showing the hydride region of a quenched sample revealing the conversion of **2** to **3**. (b) NMR spectrum showing that the aromatic region no longer exhibits SABRE while weak PHIP is seen in the hydride region of the quenched sample for the minor isomer of **3**.

sFigure 1a shows the hydride region of an NMR spectrum for a bpy quenched sample. Complete conversion of **2** into **3** is indicated. The hydride signals at  $\delta$  -19.29 ( $J_{\text{HH}} = -8$  Hz) and at  $\delta$  -23.00 ( $J_{\text{HH}} = -8$  Hz) are due to a minor isomer of **3** where the hydrides are *trans* to nicotinamide and bpy. They occur at ca. 4% of the level of the main isomer. After a shake and sample introduction, a new NMR

spectrum was obtained with a 45 degree angle. While the hydride signals of the minor isomer show PHIP no SABRE enhancement of nicotinamide is seen.

### 3. Characterisation data for cation 4

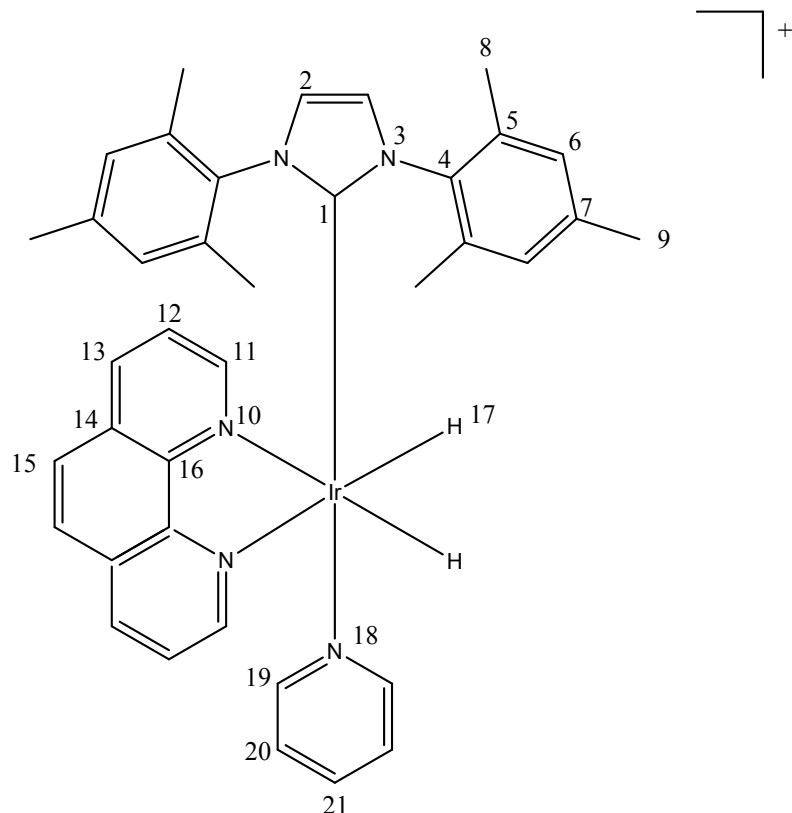
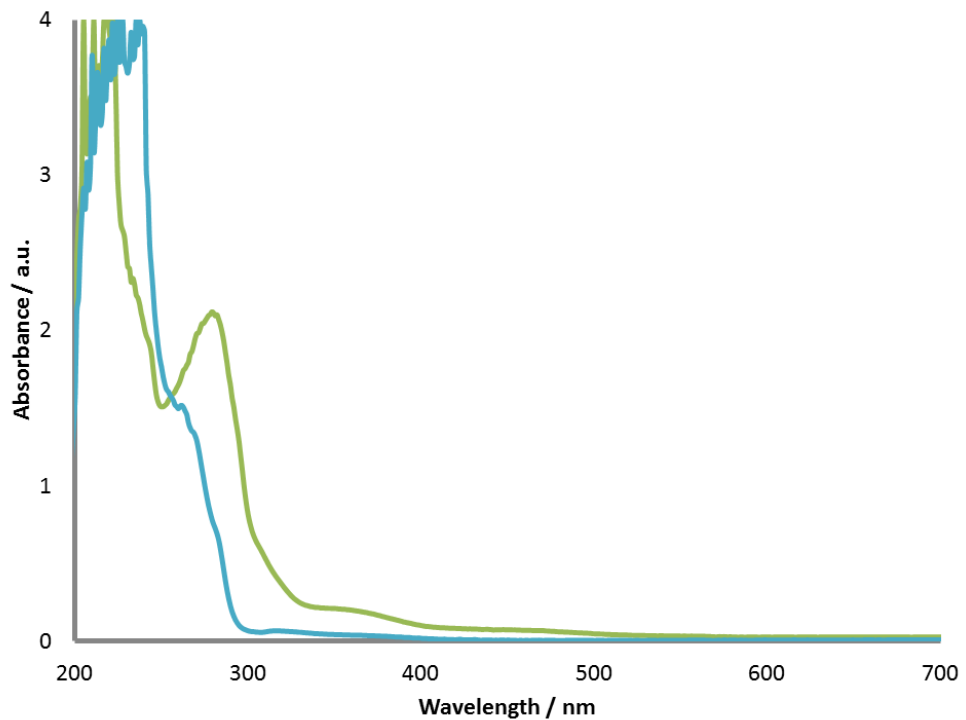


Table 2: NMR Chemical shift and spin-spin coupling data for **4**, collected in MeOH-*d*<sub>4</sub> solution at 298 K.

Atom number	<sup>1</sup> H δ /ppm	<i>J</i> <sub>HH</sub> / Hz	<sup>13</sup> C δ /ppm	<sup>15</sup> N δ /ppm
1				
2	6.93 (s)		122.5	
3				108.3
4			137.3	
5			135.4	
6	6.67 (s)		128.3	
7			138.2	
8	1.81 (s)		16.8	
9	2.26 (s)		19.8	
10				165.9
11	9.07 (d)	4.85	155.6	
12	7.80 (dd)	4.85, 8.2	126.0	
13	8.57 (d)	8.2	136.5	
14			130.7	
15	8.00		127.2	
16			148.1	
17	-20.00			
18				239.1
19	8.18 (m)	6.0	153.3	

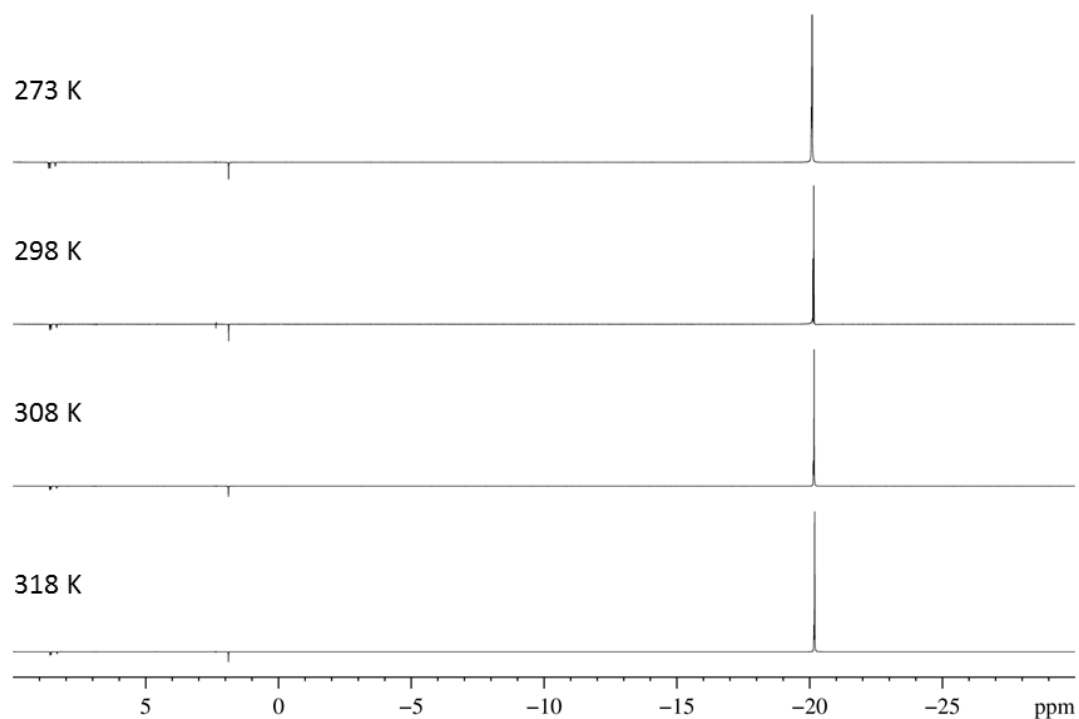
20	6.79 (dd)	7.5, 6.0	124.8	
21	7.41 (m)	7.5	136.2	

#### 4. UV-vis data for 2 and 3



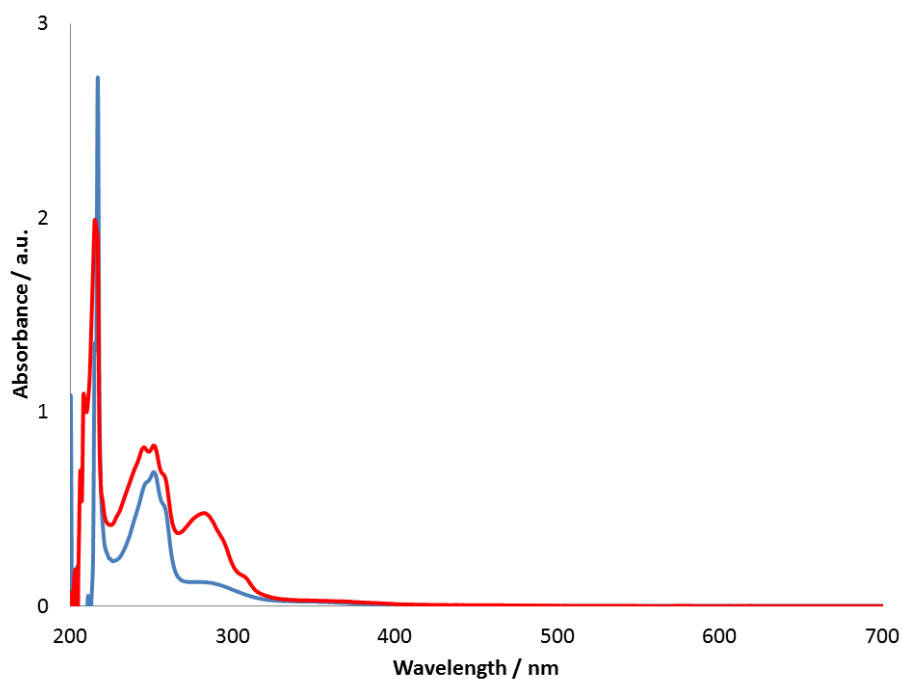
sFigure 2: UV-vis spectra of **2** (—) and **3** (—).

## 5. Selective NOESY data for $[\text{Ir}(\text{IMes})(\text{H})_2(\text{bpy})\text{L}^2]\text{Cl}$ (3)



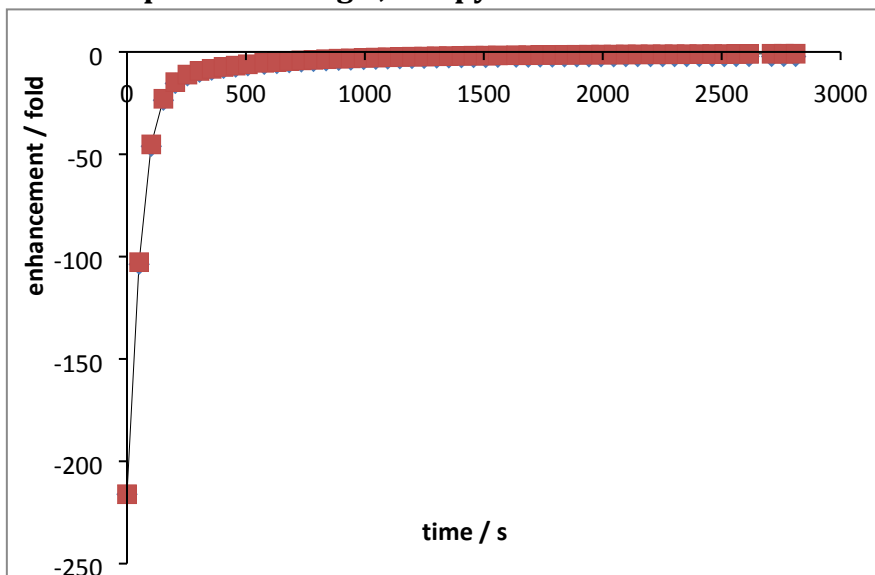
sFigure 3: Selective  $^1\text{H}$  NMR NOESY spectra showing the effect of exciting the hydride resonance at  $\delta$  -20.15 for **3** at different temperatures. No exchange peaks are visible.

## 6. UV-vis data following the change after the addition of bpy to solution of $\text{L}^2$ and 2



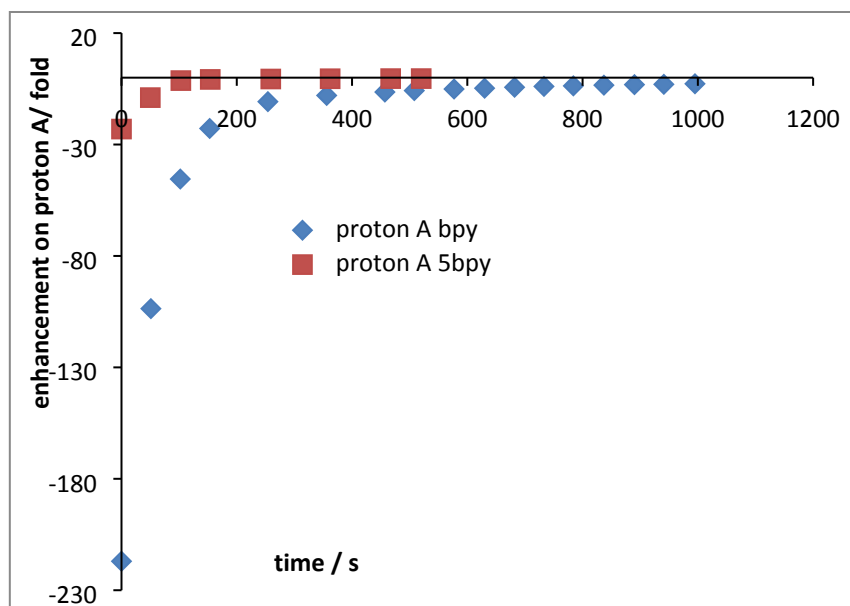
sFigure 4: UV-vis spectra of  $[\text{Ir}(\text{IMes})(\text{L}^2)_3(\text{H})_2]\text{Cl}$  (2) (—) and  $[\text{Ir}(\text{IMes})(\text{bpy})(\text{L}^2)(\text{H})_2]\text{Cl}$  (3) (—).

**7. Change in the NMR signal enhancement level seen for the bulk nicotinamide proton adding 2,2'-bipyridine as a function of time.**

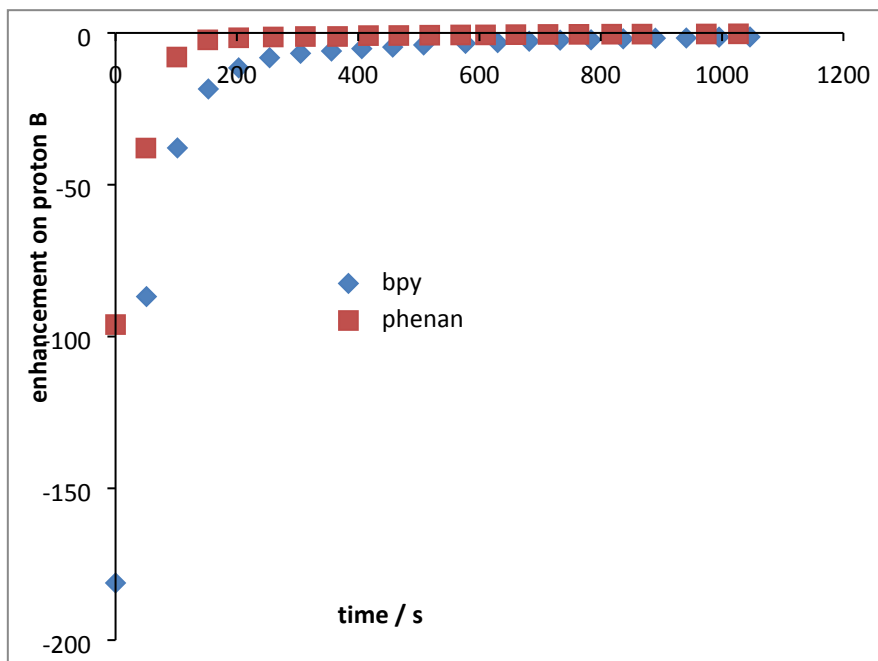


sFigure 5: Change in the nicotinamide proton signal enhancement values after the addition of 1.1 equivalents (relative to nicotinamide) of 2,2'-bipyridine to a sample consisting of **1** (10 mg) and nicotinamide (15 mg) in 3 mL of MeOD solution.

We note that the hyperpolarised control sample observed 6 seconds after polarisation transfer and the quenched sample, six seconds after transfer result in similar signal intensities of the H<sub>a</sub> resonance of nicotinamide.

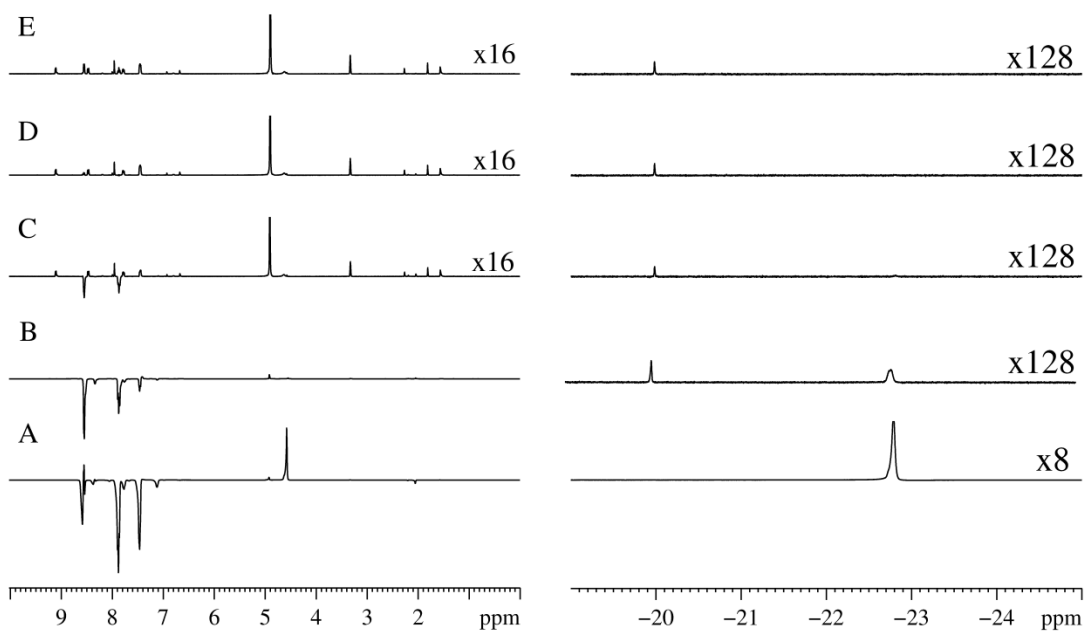


sFigure 6: Comparison in the signal enhancement decay for nicotinamide proton A with time after the addition of 1.1 (blue) and 5.1 equivalents (red), relative to nicotinamide, of 2,2'-bipyridine to a sample of **1** (10 mg) and nicotinamide (15 mg) under Hin 3 mL of MeOD solution.



sFigure 7: Comparative traces showing the signal enhancement decay of the nicotinamide proton A signal with time after the addition of 1,10-phenanthroline (red) or 1,10-phenanthroline (blue) to samples consisting of **1** (10 mg) and nicotinamide (15 mg) in 3 mL of MeOD solution.

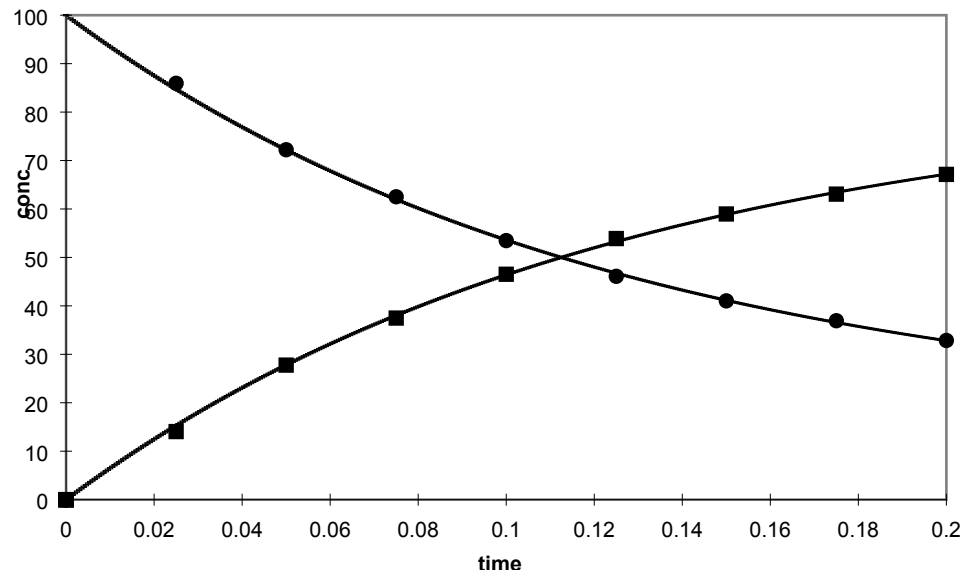
## 8. Addition of 1,10-phenanthroline to a sample consisting of **1** and pyridine



sFigure 8: Series of NMR spectra showing how the addition of 1,10-phenanthroline to a sample consisting of **1** (2 mg) and pyridine (1  $\mu$ L) in MeOD effects both speciation and hyperpolarisation effects. Trace A is prior to 1,10-phenanthroline addition and reflects the trace after the sample has been shaken in a PTF of 65 G. Trace B was obtained with a 5 degree pulse following the sample being shaken at a PTF of 65 G and then 1,10-phenanthroline (4 mg) added in a minimal amount

of MeOD. Traces C-E were collected after B, without the sample being reshaken, degassed or removed from the magnet. The total time elapsed between the acquiring of traces B and E is 94 s.

## 9. Kinetic data for the exchange of nicotinamide in 2



sFigure 9: Raw data and fitted data for ligand exchange in 2

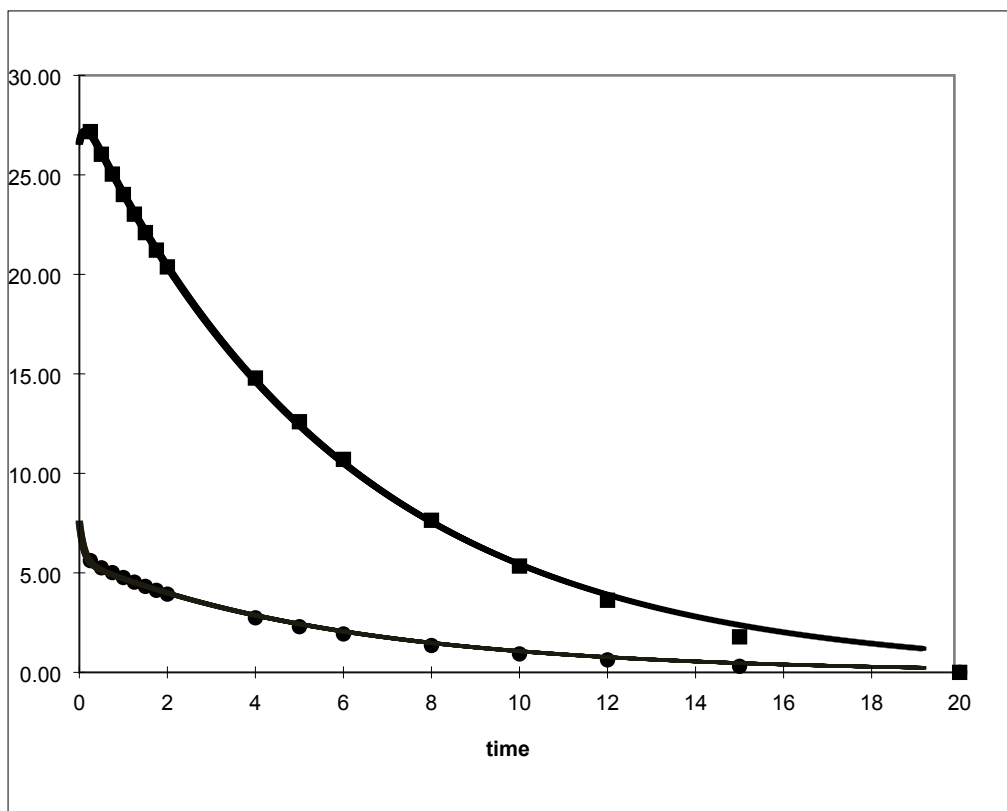
sTable 4 EXSY data for nicotinamide dissociation in 2

time(t)	Experimental data		Fitted data	
	[A]	[B]	[A]	[B]
0	0.00	100.00	0.00	100.00
0.025	14.05	85.95	15.29	84.71
0.05	27.77	72.23	27.80	72.20
0.075	37.48	62.52	38.03	61.97
0.1	46.53	53.47	46.40	53.60
0.125	53.90	46.10	53.25	46.75
0.15	58.97	41.03	58.85	41.15
0.175	63.07	36.93	63.43	36.57
0.2	67.14	32.86	67.18	32.82

Kinetic parameters used in the fit

$$k_{(AB)} = 1.28 \text{ s}^{-1} \text{ and } k_{(BA)} = 6.74 \pm 0.07 \text{ s}^{-1}$$

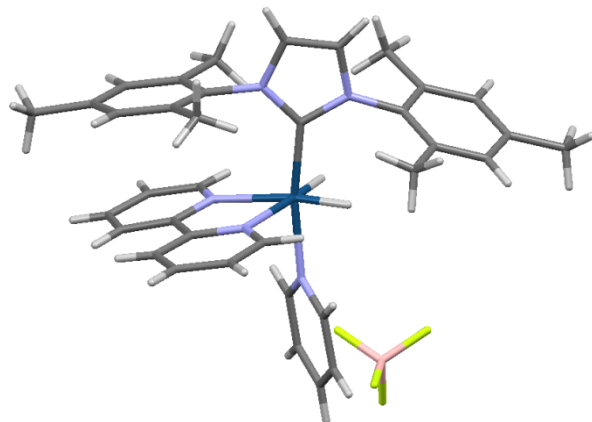
Here,  $k_{BA}$  is the rate of nicotinamide dissociation. The data was obtained by EXSY and used the mixing times indicated.



sFigure 10: Raw  $T_1$  relaxation data and simulated data for resonance Ha, free (■) and bound (●) of nicotinamide in the presence of **2** and  $H_2$ .

Values of  $k_{(AB)} = 1.46 \text{ s}^{-1}$  and  $k_{(BA)} = 6.74 \text{ s}^{-1}$ ,  $T_{1(\text{free})} 39.94$  and  $T_{1(\text{bound})} 1.13 \text{ s}$  were used in the simulation which was based on the procedure of Bain.<sup>6</sup>

## 10. Crystallographic data for 3



sFigure 10. X-Ray Crystallography structure of **3**



sTable 4: Key bond angles and distances in **3**

Bond distances (Å)			
H1-Ir	1.351	N2 <sub>bpy</sub> -Ir	2.156
H2-Ir	1.440	N3 <sub>py</sub> -Ir	2.110
N1 <sub>bpy</sub> -Ir	2.151	C1-Ir	1.981
Bond Angles			
H1-Ir-H2	84.39		
N1 <sub>bpy</sub> -Ir-N2 <sub>bpy</sub>	75.78		
H1-Ir-N1 <sub>bpy</sub>	100.56		
H2-Ir-N2 <sub>bpy</sub>	99.16		
N1 <sub>bpy</sub> -Ir-C	103.92		
N2 <sub>bpy</sub> -Ir-C	95.62		
N3 <sub>py</sub> -Ir-C	170.15		

sTable 5: Crystal data and structure refinement for **3**

Empirical formula	C48H51BF4IrN5
Formula weight	976.94
Temperature/K	110.05(10)
Crystal system	triclinic
Space group	P-1
a/Å	10.3919(3)
b/Å	13.6438(4)
c/Å	15.4722(6)
α/°	95.673(3)
β/°	95.753(3)
γ/°	98.925(3)

Volume/Å <sup>3</sup>	2141.59(12)
Z	2
ρcalcg/cm <sup>3</sup>	1.515
μ/mm <sup>-1</sup>	3.175
F(000)	984.0
Crystal size/mm <sup>3</sup>	0.2126 × 0.1703 × 0.1364
Radiation	MoKα ( $\lambda = 0.7107$ )
2θ range for data collection/°	6.702 to 60.732
Index ranges	-12 ≤ h ≤ 14, -19 ≤ k ≤ 18, -20 ≤ l ≤ 20
Reflections collected	22046
Independent reflections	11269 [Rint = 0.0346, Rsigma = 0.0596]
Data/restraints/parameters	11269/54/553
Goodness-of-fit on F <sup>2</sup>	1.067
Final R indexes [ $ I >=2\sigma(I)$ ]	R1 = 0.0331, wR2 = 0.0663
Final R indexes [all data]	R1 = 0.0408, wR2 = 0.0713
Largest diff. peak/hole / e Å <sup>-3</sup>	1.44/-0.93

sTable 6: Fractional Atomic Coordinates (×104) and Equivalent Isotropic Displacement Parameters (Å<sup>2</sup>×103) for sbd1505. Ueq is defined as 1/3 of the trace of the orthogonalised UIJ tensor.

Atom	x	y	z	U(eq)
C1	5117(3)	2632(2)	3208(2)	15.5(6)
C2	2892(3)	2395(2)	3206(2)	21.0(7)
C3	3388(3)	2046(2)	3921(2)	20.5(7)
C4	3727(3)	3055(2)	1908(2)	16.9(6)
C5	3396(3)	2303(2)	1209(2)	21.5(7)
C6	3114(3)	2588(3)	376(2)	26.9(8)
C7	3206(4)	3580(3)	236(2)	27.3(8)
C8	3568(3)	4303(3)	948(2)	22.1(7)
C9	3805(3)	4060(2)	1798(2)	18.2(7)
C10	3365(4)	1218(3)	1344(3)	34.2(9)
C11	2925(4)	3863(3)	-674(2)	40.8(10)
C12	4107(3)	4873(2)	2552(2)	22.9(7)
C13	5582(3)	1822(2)	4556(2)	15.5(6)
C14	5915(3)	2357(2)	5381(2)	18.3(7)
C15	6749(3)	1985(2)	5983(2)	20.5(7)
C16	7223(3)	1103(2)	5779(2)	19.7(7)
C17	6814(3)	563(2)	4965(2)	19.0(7)
C18	5987(3)	905(2)	4341(2)	17.7(7)
C19	5389(4)	3299(2)	5633(2)	25.0(8)
C20	8173(4)	743(2)	6428(2)	26.8(8)
C21	5536(3)	308(2)	3465(2)	22.3(7)
C22	8428(3)	1390(2)	3206(2)	18.6(7)
C23	9328(3)	906(2)	3624(2)	21.7(7)
C24	9977(3)	1329(2)	4430(2)	22.0(7)

C25	9704(3)	2231(2)	4789(2)	20.1(7)
C26	8770(3)	2676(2)	4346(2)	15.5(6)
C27	8429(3)	3642(2)	4685(2)	15.0(6)
C28	8938(3)	4142(2)	5500(2)	20.2(7)
C29	8597(3)	5057(2)	5756(2)	22.2(7)
C30	7747(4)	5450(2)	5196(2)	23.2(7)
C31	7257(3)	4909(2)	4395(2)	18.4(7)
C32	8815(3)	4838(2)	2449(2)	18.9(7)
C33	9858(3)	5345(2)	2099(2)	22.6(7)
C34	10711(3)	4812(3)	1711(2)	24.5(8)
C35	10490(3)	3782(2)	1681(2)	21.7(7)
C36	9429(3)	3329(2)	2050(2)	17.1(6)
Ir1	6881.7(2)	3144.2(2)	2899.3(2)	13.71(4)
N1	3937(3)	2749.3(18)	2769.4(17)	16.8(6)
N2	4735(3)	2183.6(18)	3917.3(18)	17.3(6)
N3	8127(3)	2258.1(17)	3561.0(17)	14.8(5)
N4	7572(3)	4016.0(17)	4141.1(16)	14.8(5)
N5	8591(3)	3837.0(19)	2429.6(17)	17.1(6)
C43	7481(18)	-628(14)	1526(18)	39.2(15)
C43A	7335(12)	-568(10)	1490(12)	39.2(15)
C48A	6851(9)	167(8)	1055(10)	45(3)
C47A	7692(11)	832(5)	660(5)	40(2)
C46A	9016(10)	762(5)	698(5)	47(2)
C45A	9500(8)	27(7)	1132(7)	49(2)
C44A	8659(12)	-638(8)	1528(10)	42.2(19)
C44	8770(20)	-422(13)	1442(16)	42.2(19)
C45	9228(17)	386(11)	1022(11)	49(2)
C46	8360(18)	891(11)	635(10)	47(2)
C47	6987(15)	695(10)	712(8)	40(2)
C48	6581(18)	-127(13)	1166(15)	45(3)
C37	6484(4)	3146(3)	-178(3)	39.6(10)
C38	7837(4)	3430(3)	-7(3)	34.3(9)
C39	8647(5)	3085(3)	-572(3)	44.1(11)
C40	8124(6)	2449(3)	-1312(3)	56.2(14)
C41	6770(6)	2179(4)	-1488(3)	65.5(17)
C42	5963(5)	2534(3)	-923(3)	53.4(13)
B1	7848(5)	7606(3)	3238(3)	32.2(10)
F1	8921(3)	7629(3)	2777(3)	101.5(13)
F2	8036(4)	8448(2)	3792(2)	94.2(13)
F3	6723(3)	7491(2)	2690.9(16)	53.3(7)
F4	7878(4)	6792(2)	3669(2)	90.8(12)

sTable 7: Anisotropic Displacement Parameters ( $\text{\AA}^2 \times 103$ ) for sbd1505. The Anisotropic displacement factor exponent takes the form:  $-2\pi^2[h2a^*2U11+2hka^*b^*U12+\dots]$ .

Atom	U11	U22	U33	U23	U13	U12
C1	17.2(16)	11.8(13)	16.3(16)	-4.4(11)	1.2(13)	3.0(12)
C2	12.7(16)	23.3(16)	25.8(19)	-0.8(13)	2.3(14)	1.8(13)
C3	14.8(16)	21.8(16)	25.4(19)	1.7(13)	5.4(14)	3.4(13)
C4	11.5(15)	23.6(16)	15.0(16)	0.3(12)	-0.9(12)	4.3(13)
C5	16.6(16)	26.1(17)	19.8(18)	-6.1(13)	1.0(13)	3.9(14)
C6	23.1(19)	35.6(19)	19.4(19)	-9.1(14)	-1.4(15)	6.9(16)
C7	22.4(18)	43(2)	17.2(18)	0.9(15)	-1.7(14)	12.1(17)
C8	14.8(16)	31.4(18)	22.4(18)	5.9(14)	1.5(14)	9.3(14)
C9	11.6(15)	26.0(16)	15.9(16)	-1.7(12)	0.2(12)	3.7(13)
C10	37(2)	27.2(19)	35(2)	-7.3(16)	-2.8(18)	5.1(17)
C11	47(3)	57(3)	19(2)	1.7(18)	-4.5(18)	17(2)
C12	24.3(18)	22.2(16)	21.5(18)	-1.7(13)	-1.0(14)	6.9(14)
C13	14.3(15)	16.9(14)	16.1(16)	3.3(12)	3.9(12)	2.7(12)
C14	17.6(16)	19.2(15)	19.7(17)	2.4(12)	7.5(13)	4.1(13)
C15	20.2(17)	23.7(16)	17.1(17)	1.2(13)	1.9(13)	3.0(14)
C16	15.9(16)	20.3(15)	24.2(18)	8.8(13)	2.5(14)	3.0(13)
C17	19.2(17)	13.7(14)	26.5(19)	4.8(12)	6.0(14)	6.4(13)
C18	15.0(16)	18.1(15)	20.3(17)	3.3(12)	6.6(13)	-0.3(13)
C19	30(2)	23.0(17)	23.6(19)	0.6(14)	4.7(15)	10.9(15)
C20	24.1(19)	24.4(17)	32(2)	4.3(15)	-1.3(16)	6.6(15)
C21	24.0(18)	19.8(16)	22.1(18)	-0.3(13)	4.9(14)	1.0(14)
C22	18.1(16)	14.6(14)	22.4(18)	-0.5(12)	2.8(13)	2.3(13)
C23	21.1(17)	17.9(15)	28.6(19)	3.0(13)	6.2(15)	8.8(14)
C24	19.2(17)	22.0(16)	28(2)	7.3(14)	5.1(14)	10.0(14)
C25	17.1(16)	24.2(16)	19.8(17)	5.9(13)	2.5(13)	4.2(14)
C26	13.3(15)	15.5(14)	18.2(16)	1.9(12)	2.6(12)	3.1(12)
C27	13.2(15)	15.5(14)	15.7(16)	1.3(11)	0.7(12)	1.9(12)
C28	20.7(17)	20.3(15)	18.7(17)	2.6(12)	-1.4(14)	3.2(14)
C29	24.3(18)	20.2(16)	19.0(18)	-5.1(13)	-1.8(14)	1.3(14)
C30	28.3(19)	18.7(15)	22.8(19)	-1.9(13)	2.7(15)	7.2(14)
C31	17.0(16)	16.6(15)	22.1(18)	0.8(12)	0.6(13)	6.7(13)
C32	18.9(17)	20.9(15)	17.6(17)	3.2(12)	0.1(13)	6.2(13)
C33	21.8(18)	22.2(16)	22.9(18)	6.2(13)	-0.5(14)	0.6(14)
C34	16.6(17)	33.9(19)	24.7(19)	12.3(15)	2.8(14)	3.6(15)
C35	15.7(16)	32.0(18)	18.8(17)	1.8(14)	3.7(13)	7.9(14)
C36	16.8(16)	21.9(15)	12.6(16)	0.3(12)	0.0(12)	5.6(13)
Ir1	12.28(6)	15.26(6)	13.06(7)	-0.26(4)	-0.41(4)	3.09(4)
N1	14.5(13)	18.6(13)	16.0(14)	-2.2(10)	1.2(11)	1.6(11)
N2	14.6(13)	17.5(12)	19.4(15)	2.4(10)	1.0(11)	2.2(11)
N3	12.9(13)	13.2(12)	18.6(14)	0.9(10)	3.2(11)	2.3(10)
N4	17.1(13)	14.4(12)	12.7(13)	0.8(9)	1(1)	2.6(11)
N5	13.4(13)	22.8(13)	14.4(14)	1.4(10)	0.0(11)	2.3(11)
C43	53(4)	31(3)	28(3)	-8.9(18)	0(3)	-2(3)
C43A	53(4)	31(3)	28(3)	-8.9(18)	0(3)	-2(3)
C48A	74(6)	29(7)	28(5)	-10(5)	-4(4)	11(5)
C47A	53(5)	35(3)	30(3)	-7(2)	-4(4)	16(5)
C46A	71(6)	38(3)	30(3)	2(2)	11(4)	-2(4)

C45A	61(4)	37(5)	50(4)	-2(4)	21(3)	7(4)
C44A	62(4)	25(5)	37(4)	-9(3)	8(3)	5(4)
C44	62(4)	25(5)	37(4)	-9(3)	8(3)	5(4)
C45	61(4)	37(5)	50(4)	-2(4)	21(3)	7(4)
C46	71(6)	38(3)	30(3)	2(2)	11(4)	-2(4)
C47	53(5)	35(3)	30(3)	-7(2)	-4(4)	16(5)
C48	74(6)	29(7)	28(5)	-10(5)	-4(4)	11(5)
C37	39(3)	38(2)	42(3)	7.9(18)	0(2)	9(2)
C38	39(2)	38(2)	27(2)	9.2(16)	-3.1(18)	10.1(19)
C39	43(3)	49(3)	42(3)	15(2)	7(2)	6(2)
C40	70(4)	54(3)	43(3)	2(2)	29(3)	-7(3)
C41	86(4)	64(3)	33(3)	-3(2)	11(3)	-29(3)
C42	50(3)	58(3)	43(3)	8(2)	-3(2)	-16(3)
B1	32(2)	25(2)	38(3)	10.4(18)	-4(2)	-0.8(19)
F1	45(2)	140(3)	111(3)	-7(2)	21(2)	-5(2)
F2	99(3)	63.8(19)	106(3)	-42.5(18)	-56(2)	45.1(19)
F3	41.7(15)	70.7(17)	41.5(16)	3.0(13)	-14.1(12)	5.1(14)
F4	107(3)	52.6(17)	102(3)	43.7(17)	-36(2)	-12.1(18)

sTable 8: Bond Lengths for **3**

Atom	Atom	Length/Å	Atom	Atom	Length/Å
C1	Ir1	1.981(3)	C28	C29	1.382(4)
C1	N1	1.381(4)	C29	C30	1.380(5)
C1	N2	1.371(4)	C30	C31	1.384(4)
C2	C3	1.335(5)	C31	N4	1.341(4)
C2	N1	1.385(4)	C32	C33	1.381(4)
C3	N2	1.384(4)	C32	N5	1.347(4)
C4	C5	1.391(4)	C33	C34	1.376(5)
C4	C9	1.389(4)	C34	C35	1.383(5)
C4	N1	1.441(4)	C35	C36	1.382(4)
C5	C6	1.399(5)	C36	N5	1.339(4)
C5	C10	1.512(5)	Ir1	N3	2.156(3)
C6	C7	1.382(5)	Ir1	N4	2.151(2)
C7	C8	1.383(5)	Ir1	N5	2.110(3)
C7	C11	1.509(5)	C43	C44	1.344(16)
C8	C9	1.397(5)	C43	C48	1.349(17)
C9	C12	1.501(4)	C43A	C48A	1.3900
C13	C14	1.389(4)	C43A	C44A	1.3900
C13	C18	1.401(4)	C48A	C47A	1.3900
C13	N2	1.432(4)	C47A	C46A	1.3900
C14	C15	1.395(4)	C46A	C45A	1.3900
C14	C19	1.505(4)	C45A	C44A	1.3900
C15	C16	1.388(5)	C44	C45	1.381(19)
C16	C17	1.388(5)	C45	C46	1.35(2)
C16	C20	1.508(4)	C46	C47	1.429(17)
C17	C18	1.391(4)	C47	C48	1.413(17)
C18	C21	1.502(4)	C37	C38	1.390(6)
C22	C23	1.373(4)	C37	C42	1.364(6)
C22	N3	1.351(4)	C38	C39	1.372(6)

C23	C24	1.382(5)	C39	C40	1.376(6)
C24	C25	1.381(4)	C40	C41	1.390(7)
C25	C26	1.383(4)	C41	C42	1.376(7)
C26	C27	1.478(4)	B1	F1	1.379(6)
C26	N3	1.353(4)	B1	F2	1.340(5)
C27	C28	1.385(4)	B1	F3	1.352(5)
C27	N4	1.357(4)	B1	F4	1.354(5)

sTable 9: Bond Angles for **3**.

Atom	Atom	Atom	Angle/°	Atom	Atom	Atom	Angle/°
N1	C1	Ir1	125.9(2)	C33	C34	C35	118.8(3)
N2	C1	Ir1	131.2(2)	C36	C35	C34	118.7(3)
N2	C1	N1	102.6(3)	N5	C36	C35	123.2(3)
C3	C2	N1	107.2(3)	C1	Ir1	N3	103.37(11)
C2	C3	N2	106.9(3)	C1	Ir1	N4	95.59(11)
C5	C4	N1	117.2(3)	C1	Ir1	N5	170.16(11)
C9	C4	C5	122.3(3)	N4	Ir1	N3	75.79(9)
C9	C4	N1	120.5(3)	N5	Ir1	N3	86.42(10)
C4	C5	C6	117.7(3)	N5	Ir1	N4	87.67(10)
C4	C5	C10	121.1(3)	C1	N1	C2	111.4(3)
C6	C5	C10	121.2(3)	C1	N1	C4	126.9(3)
C7	C6	C5	121.8(3)	C2	N1	C4	121.2(3)
C6	C7	C8	118.4(3)	C1	N2	C3	111.9(3)
C6	C7	C11	120.5(3)	C1	N2	C13	125.6(3)
C8	C7	C11	121.1(3)	C3	N2	C13	122.3(3)
C7	C8	C9	122.1(3)	C22	N3	C26	118.3(3)
C4	C9	C8	117.5(3)	C22	N3	Ir1	124.9(2)
C4	C9	C12	122.6(3)	C26	N3	Ir1	116.30(19)
C8	C9	C12	119.8(3)	C27	N4	Ir1	116.6(2)
C14	C13	C18	122.0(3)	C31	N4	C27	118.4(3)
C14	C13	N2	119.4(3)	C31	N4	Ir1	124.9(2)
C18	C13	N2	118.5(3)	C32	N5	Ir1	119.1(2)
C13	C14	C15	117.7(3)	C36	N5	C32	117.4(3)
C13	C14	C19	121.9(3)	C36	N5	Ir1	123.4(2)
C15	C14	C19	120.3(3)	C44	C43	C48	123.4(12)
C16	C15	C14	121.8(3)	C48A	C43A	C44A	120.0
C15	C16	C20	120.7(3)	C47A	C48A	C43A	120.0
C17	C16	C15	118.8(3)	C48A	C47A	C46A	120.0
C17	C16	C20	120.5(3)	C45A	C46A	C47A	120.0
C16	C17	C18	121.5(3)	C46A	C45A	C44A	120.0
C13	C18	C21	120.9(3)	C45A	C44A	C43A	120.0
C17	C18	C13	118.0(3)	C43	C44	C45	119.4(13)
C17	C18	C21	121.1(3)	C46	C45	C44	118.9(13)
N3	C22	C23	122.4(3)	C45	C46	C47	123.0(13)
C22	C23	C24	119.2(3)	C48	C47	C46	115.1(13)
C25	C24	C23	118.9(3)	C43	C48	C47	119.8(15)
C24	C25	C26	119.4(3)	C42	C37	C38	119.5(5)
C25	C26	C27	122.6(3)	C39	C38	C37	120.5(4)
N3	C26	C25	121.7(3)	C38	C39	C40	120.1(5)

N3	C26	C27	115.7(3)	C39	C40	C41	119.2(5)
C28	C27	C26	123.2(3)	C42	C41	C40	120.4(5)
N4	C27	C26	115.3(3)	C37	C42	C41	120.3(5)
N4	C27	C28	121.5(3)	F2	B1	F1	107.6(4)
C29	C28	C27	119.5(3)	F2	B1	F3	112.5(4)
C30	C29	C28	119.1(3)	F2	B1	F4	111.6(4)
C29	C30	C31	118.7(3)	F3	B1	F1	111.1(4)
N4	C31	C30	122.7(3)	F3	B1	F4	110.1(3)
N5	C32	C33	122.8(3)	F4	B1	F1	103.5(4)
C34	C33	C32	119.1(3)				

sTable 10: Torsion Angles for **3**.

A	B	C	D	Angle/ <sup>°</sup>	A	B	C	D	Angle/ <sup>°</sup>
C2	C3	N2	C1	0.8(4)	C28	C27	N4	Ir1	179.9(2)
C2	C3	N2	C13	-175.0(3)	C28	C29	C30	C31	0.3(5)
C3	C2	N1	C1	-0.3(4)	C29	C30	C31	N4	0.2(5)
C3	C2	N1	C4	171.5(3)	C30	C31	N4	C27	-1.6(5)
C4	C5	C6	C7	2.4(5)	C30	C31	N4	Ir1	-178.8(2)
C5	C4	C9	C8	-1.5(5)	C32	C33	C34	C35	0.4(5)
C5	C4	C9	C12	177.4(3)	C33	C32	N5	C36	-0.1(5)
C5	C4	N1	C1	93.0(4)	C33	C32	N5	Ir1	-175.3(2)
C5	C4	N1	C2	-77.5(4)	C33	C34	C35	C36	-0.7(5)
C5	C6	C7	C8	-1.0(6)	C34	C35	C36	N5	0.6(5)
C5	C6	C7	C11	178.6(4)	C35	C36	N5	C32	-0.2(5)
C6	C7	C8	C9	-1.8(5)	C35	C36	N5	Ir1	174.7(2)
C7	C8	C9	C4	3.0(5)	Ir1	C1	N1	C2	-173.6(2)
C7	C8	C9	C12	-175.9(3)	Ir1	C1	N1	C4	15.1(4)
C9	C4	C5	C6	-1.1(5)	Ir1	C1	N2	C3	173.0(2)
C9	C4	C5	C10	177.8(3)	Ir1	C1	N2	C13	-11.4(4)
C9	C4	N1	C1	-89.5(4)	N1	C1	N2	C3	-0.9(3)
C9	C4	N1	C2	100.0(4)	N1	C1	N2	C13	174.7(3)
C10	C5	C6	C7	-176.6(3)	N1	C2	C3	N2	-0.3(4)
C11	C7	C8	C9	178.6(3)	N1	C4	C5	C6	176.3(3)
C13	C14	C15	C16	-0.9(5)	N1	C4	C5	C10	-4.7(5)
C14	C13	C18	C17	-4.0(5)	N1	C4	C9	C8	-178.8(3)
C14	C13	C18	C21	175.7(3)	N1	C4	C9	C12	0.0(5)
C14	C13	N2	C1	105.5(4)	N2	C1	N1	C2	0.7(3)
C14	C13	N2	C3	-79.4(4)	N2	C1	N1	C4	-170.5(3)
C14	C15	C16	C17	-2.4(5)	N2	C13	C14	C15	-179.6(3)
C14	C15	C16	C20	177.1(3)	N2	C13	C14	C19	1.3(5)
C15	C16	C17	C18	2.6(5)	N2	C13	C18	C17	179.8(3)
C16	C17	C18	C13	0.5(5)	N2	C13	C18	C21	-0.5(4)
C16	C17	C18	C21	-179.2(3)	N3	C22	C23	C24	-1.6(5)
C18	C13	C14	C15	4.2(5)	N3	C26	C27	C28	176.1(3)
C18	C13	C14	C19	-174.9(3)	N3	C26	C27	N4	-3.8(4)
C18	C13	N2	C1	-78.2(4)	N4	C27	C28	C29	-2.0(5)
C18	C13	N2	C3	96.9(4)	N5	C32	C33	C34	0.1(5)
C19	C14	C15	C16	178.2(3)	C43	C44	C45	C46	-6.2(17)
C20	C16	C17	C18	-176.9(3)	C43A	C48A	C47A	C46A	0.0
C22	C23	C24	C25	-0.3(5)	C48A	C43A	C44A	C45A	0.0

C23	C22	N3	C26	2.1(5)	C48A	C47A	C46A	C45A	0.0
C23	C22	N3	Ir1	173.4(2)	C47A	C46A	C45A	C44A	0.0
C23	C24	C25	C26	1.5(5)	C46A	C45A	C44A	C43A	0.0
C24	C25	C26	C27	-179.7(3)	C44A	C43A	C48A	C47A	0.0
C24	C25	C26	N3	-1.0(5)	C44	C43	C48	C47	-3.6(16)
C25	C26	C27	C28	-5.1(5)	C44	C45	C46	C47	7(2)
C25	C26	C27	N4	174.9(3)	C45	C46	C47	C48	-5(2)
C25	C26	N3	C22	-0.8(4)	C46	C47	C48	C43	3.4(17)
C25	C26	N3	Ir1	-172.8(2)	C48	C43	C44	C45	5.0(16)
C26	C27	C28	C29	178.1(3)	C37	C38	C39	C40	-0.4(6)
C26	C27	N4	C31	-177.5(3)	C38	C37	C42	C41	1.7(7)
C26	C27	N4	Ir1	-0.2(3)	C38	C39	C40	C41	1.4(7)
C27	C26	N3	C22	178.0(3)	C39	C40	C41	C42	-0.8(8)
C27	C26	N3	Ir1	6.0(3)	C40	C41	C42	C37	-0.8(8)
C27	C28	C29	C30	0.5(5)	C42	C37	C38	C39	-1.1(6)
C28	C27	N4	C31	2.5(5)					

sTable 11: Hydrogen Atom Coordinates ( $\text{\AA} \times 10^4$ ) and Isotropic Displacement Parameters ( $\text{\AA}^2 \times 10^3$ ) for **3**

Atom	x	y	z	U(eq)
H2	2010	2400	3033	25
H3	2917	1764	4342	25
H6	2859	2096	-97	32
H8	3656	4973	857	27
H10A	2722	1027	1728	51
H10B	4213	1126	1600	51
H10C	3141	810	791	51
H11A	2185	4205	-699	61
H11B	2735	3270	-1086	61
H11C	3677	4293	-817	61
H12A	4927	5287	2505	34
H12B	4166	4580	3092	34
H12C	3422	5270	2543	34
H15	6995	2336	6536	25
H17	7099	-42	4833	23
H19A	4589	3136	5887	38
H19B	5221	3627	5122	38
H19C	6022	3735	6050	38
H20A	8060	27	6340	40
H20B	8011	956	7012	40
H20C	9055	1018	6346	40
H21A	5961	-269	3416	33
H21B	5756	712	3010	33
H21C	4603	98	3409	33
H22	8011	1109	2657	22
H23	9499	301	3369	26
H24	10587	1012	4725	26
H25	10145	2536	5324	24
H28	9504	3864	5872	24

H29	8936	5404	6300	27
H30	7508	6066	5353	28
H31	6687	5175	4017	22
H32	8242	5204	2709	23
H33	9983	6038	2124	27
H34	11423	5138	1474	29
H35	11045	3403	1418	26
H36	9289	2637	2033	21
H43	7197	-1142	1850	47
H43A	6773	-1013	1755	47
H48A	5965	214	1030	54
H47A	7368	1324	369	48
H46A	9578	1207	433	57
H45A	10386	-20	1158	59
H44A	8983	-1130	1819	51
H44	9340	-820	1664	51
H45	10124	578	1007	59
H46	8667	1390	302	57
H47	6404	1080	481	48
H48	5697	-323	1215	54
H37	5939	3371	211	47
H38	8195	3856	494	41
H39	9550	3283	-455	53
H40	8670	2203	-1691	67
H41	6408	1756	-1991	79
H42	5057	2356	-1049	64
H	6520(30)	2540(20)	2140(20)	11(8)
HA	6220(30)	3840(20)	2460(20)	17(9)

sTable 12: Atomic Occupancy for **3**

Atom	Occupancy	Atom	Occupancy	Atom	Occupancy
C43	0.435(8)	H43	0.435(8)	C43A	0.565(8)
H43A	0.565(8)	C48A	0.565(8)	H48A	0.565(8)
C47A	0.565(8)	H47A	0.565(8)	C46A	0.565(8)
H46A	0.565(8)	C45A	0.565(8)	H45A	0.565(8)
C44A	0.565(8)	H44A	0.565(8)	C44	0.435(8)
H44	0.435(8)	C45	0.435(8)	H45	0.435(8)
C46	0.435(8)	H46	0.435(8)	C47	0.435(8)
H47	0.435(8)	C48	0.435(8)	H48	0.435(8)

## 11. References

1. O. Torres, M. Martin and E. Sola, *Organometallics*, 2009, 28, 863-870.
2. R. E. Mewis, K. D. Atkinson, M. J. Cowley, S. B. Duckett, G. G. R. Green, R. A. Green, L. A. R. Highton, D. Kilgour, L. S. Lloyd, J. A. B. Lohman and D. C. Williamson, *Magn. Reson. Chem.*, 2014, 52, 358-369.
3. Dolomanov, O.V., Bourhis, L.J., Gildea, R.J., Howard, J.A.K. & Puschmann, H. (2009), *J. Appl. Cryst.* 42, 339-341.
4. Palatinus, L. & Chapuis, G. (2007). *J. Appl. Cryst.*, 40, 786-790; Palatinus, L. & van der Lee, A. (2008). *J. Appl. Cryst.* 41, 975-984; Palatinus, L., Prathapa, S. J. & van Smaalen, S. (2012). *J. Appl. Cryst.* 45, 575-580.

5. Sheldrick, G.M. (2008). *Acta Cryst. A*64, 112-122.
6. Bain, A. D., Chemical Exchange in Nmr. *Prog. Nucl. Magn. Reson. Spectrosc.* **2003**, 43, 63-103.